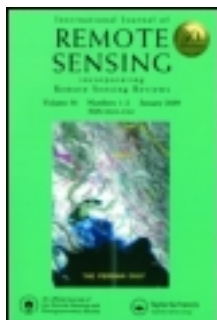


This article was downloaded by: [University of California, Los Angeles (UCLA)]

On: 24 July 2013, At: 21:56

Publisher: Taylor & Francis

Informa Ltd Registered in England and Wales Registered Number: 1072954 Registered office: Mortimer House, 37-41 Mortimer Street, London W1T 3JH, UK



International Journal of Remote Sensing

Publication details, including instructions for authors and subscription information:

<http://www.tandfonline.com/loi/tres20>

An improved topographic mapping technique from airborne lidar: application in a forested hillside

Jun-Hak Lee ^a, Gregory S. Biging ^a, John D. Radke ^b & Joshua B. Fisher ^c

^a Department of Environmental Science, Policy and Management, University of California, Berkeley, CA, USA

^b Department of Landscape Architecture and Environmental Planning, University of California, Berkeley, CA, USA

^c Jet Propulsion Laboratory, California Institute of Technology, Pasadena, CA, USA

Published online: 24 Jul 2013.

To cite this article: Jun-Hak Lee, Gregory S. Biging, John D. Radke & Joshua B. Fisher (2013) An improved topographic mapping technique from airborne lidar: application in a forested hillside, International Journal of Remote Sensing, 34:20, 7293-7311, DOI: [10.1080/01431161.2013.817710](https://doi.org/10.1080/01431161.2013.817710)

To link to this article: <http://dx.doi.org/10.1080/01431161.2013.817710>

PLEASE SCROLL DOWN FOR ARTICLE

Taylor & Francis makes every effort to ensure the accuracy of all the information (the "Content") contained in the publications on our platform. However, Taylor & Francis, our agents, and our licensors make no representations or warranties whatsoever as to the accuracy, completeness, or suitability for any purpose of the Content. Any opinions and views expressed in this publication are the opinions and views of the authors, and are not the views of or endorsed by Taylor & Francis. The accuracy of the Content should not be relied upon and should be independently verified with primary sources of information. Taylor and Francis shall not be liable for any losses, actions, claims, proceedings, demands, costs, expenses, damages, and other liabilities whatsoever or howsoever caused arising directly or indirectly in connection with, in relation to or arising out of the use of the Content.

This article may be used for research, teaching, and private study purposes. Any substantial or systematic reproduction, redistribution, reselling, loan, sub-licensing, systematic supply, or distribution in any form to anyone is expressly forbidden. Terms &

Conditions of access and use can be found at <http://www.tandfonline.com/page/terms-and-conditions>

An improved topographic mapping technique from airborne lidar: application in a forested hillside

Jun-Hak Lee^{a*}, Gregory S. Biging^a, John D. Radke^b, and Joshua B. Fisher^c

^aDepartment of Environmental Science, Policy and Management, University of California, Berkeley, CA, USA; ^bDepartment of Landscape Architecture and Environmental Planning, University of California, Berkeley, CA, USA; ^cJet Propulsion Laboratory, California Institute of Technology, Pasadena, CA, USA

(Received 30 March 2012; accepted 27 May 2013)

We developed a robust method to reconstruct a digital terrain model (DTM) by classifying raw light detection and ranging (lidar) points into ground and non-ground points with the help of the Progressive Terrain Fragmentation (PTF) method. PTF applies iterative steps for searching terrain points by approximating terrain surfaces using the triangulated irregular network (TIN) model constructed from ground return points. Instead of using absolute slope or offset distance, PTF uses orthogonal distance and relative angle between a triangular plane and a node. Due to this characteristic, PTF was able to classify raw lidar points into ground and non-ground points on a heterogeneous steep forested area with a small number of parameters. We tested this approach by using a lidar data set covering a part of the Angelo Coast Range Reserve on the South Fork of the Eel River in Mendocino County, California, USA. We used systematically positioned 16 reference plots to determine the optimal parameter that can be used to separate ground and non-ground points from raw lidar point clouds. We tested at different admissible hillslope angles (15° to 20°), and the minimum total error (1.6%) was acquired at the angle value of 18°. Because classifying raw lidar points into ground and non-ground points is the basis for other types of analyses, we expect that our study will provide more accurate terrain approximation and contribute to improving the extraction of other forest biophysical parameters.

1. Introduction

Using airborne light detection and ranging (lidar) for topographic mapping is rapidly becoming standard practice in geo-spatial science because lidar is one of the most effective methods for extracting three-dimensional (3D) shapes in a terrestrial environment (Hodgson and Bresnahan 2004; Liu 2008). Lidar is used in hydrological modelling, coastal management, urban planning, landscape ecology, and forest management (Lefsky et al. 2002; Lim et al. 2003; Wulder et al. 2008). Compared with traditional airborne data (such as optical images and multispectral images), which typically provide only horizontal information, lidar directly provides both horizontal and vertical information (Lim et al. 2003). Subsequently, lidar is very effective for quantitative assessment of forest parameters because it is able to directly depict 3D object shapes by capturing high-density and high-accuracy 3D point clouds in object space (Habib et al. 2005). Because the lidar beam has the

*Corresponding author. Email: jhlee@berkeley.edu

ability to pass through gaps in foliage and reflect from different parts of a forest canopy, several studies have used lidar data to extract forest biophysical parameters such as tree height, timber volume, and forest biomass over extensive forested areas (Asner et al. 2011; Clark et al. 2011; Jensen et al. 2006; Lee and Lucas 2007; Næsset et al. 2004; Popescu 2007; Wulder et al. 2008). Forest measurement by airborne laser scanning requires a digital terrain model (DTM) for representing the ground surface and a digital surface model (DSM) for describing the canopy surface (Hyypä et al. 2008). Thus, creating an accurate terrain surface is critical for accurate forest parameter estimation because an incorrect terrain surface model propagates the error to its derivatives in forest parameter estimation.

Even though airborne laser scanning provides highly accurate 3-D point clouds representing surface shapes in great detail, there is no distinction in raw lidar points in regard to whether a point represents a terrain or a non-terrain object. It is a prerequisite to separate clouds of lidar points into ground returns and non-ground returns in almost all of the applications using airborne laser scanning (Evans and Hudak 2007). Accordingly, efficient and accurate ground filtering is critical in using airborne laser scanning across disciplines. Although terrain surface extraction is an essential part of processing lidar data, it is surprisingly difficult to extract accurate terrain surface from raw lidar point clouds because the data represent multiple surface objects over the complex terrain surface, and there is a broad range of studies for extracting bare earth surface from lidar data (Liu 2008).

Sithole and Vosselman (2004) used four categories including slope-based, block-minimum, surface-based, and clustering/segmentation methods and discussed characteristics of each approach. Liu (2008) used slightly different categories to review several research studies and addressed interpolation-based, slope-based, and morphological methods as the most popular approaches.

The slope-based method developed by Vosselman (2000) used an assumption that the gradient of natural ground slope is distinctly different from the slope of non-ground objects such as trees and buildings to separate ground and non-ground points (Sithole 2001). Vosselman's method is only applicable for gently sloped areas because a single static gradient threshold fails to distinguish terrain slope *versus* non-terrain object when the terrain has steep slopes. Sithole (2001) modified previous methods so that the threshold changes with the terrain slopes. However, this method still has limited filtering performance in areas with large buildings or low vegetation penetration.

Interpolation-based methods, first proposed by Kraus and Pfeifer (1998), iteratively approximate the ground using weighted linear least squares interpolation. This method creates a rough approximation of the terrain surface and uses it to calculate residuals (offset between the points and the surface). Based on calculated residual, different weights are assigned to each point. Points of negative residual are more likely to be ground points than the others so that more weight is assigned for points of negative residuals to calculate terrain interpolation. Lee and Younan (2003) enhanced Kraus and Pfeifer's method by implementing adaptive line enhancement (ALE) – substituting the least squares method with normalized least squares so that it creates a robust terrain surface even for steep slopes or spurious peaks. However, the ALE method needs a number of parameters (delay factor and adaptation parameters) and relatively subjective trial and error procedures are still required to select appropriate parameters.

Morphological methods are relatively simple and fast, so they have an advantage in processing large amounts of lidar points. Defining optimal operator size is the key factor in creating a correct terrain surface – removing non-ground objects, yet keeping the shape of the terrain surface. However, it is almost impossible to meet this demand with one fixed window size. Kilian, Haala, and Englich (1996) applied the morphological operator

(opening) several times with different operator sizes starting from the smallest window size. Then each point was assigned different weights proportional to the window size when it was classified as a ground point. Zhang et al. (2003) suggested progressive use of morphological filters to remove non-ground features by gradually increasing the window size of the filter, and the thresholds were determined by the elevation difference between surfaces before and after filtering. This method assumed the slope is constant. However, the major limitation of this method is that a constant slope over the area is not a realistic condition, especially in complex environments. Chen (2007) improved the method of Zhang et al. (2003) in that their method does not require the assumption of a constant slope. They used the fact that non-terrain objects (such as buildings) normally have sudden elevation changes along the edges, but the change of ground is usually not abrupt like non-terrain objects. This method shows encouraging results compared with other methods with minimum requirements for parameters and assumptions. In general, this method performs well, but when lidar points do not have enough penetration through vegetation (such as in old and densely forested areas), this method can create false flat-terrain surfaces under large trees in steep-terrain areas.

The block-minimum (or local minimum) method is relatively simple. This method searches for the minimum value from the neighbour points within a given spatial extent (Clark, Clark, and Roberts 2004; Cobby, Mason, and Davenport 2001; Suarez et al. 2005). Even though the idea is simple, it is almost impossible to find one filter size that removes all non-terrain objects without compromising for details of the terrain surface. Wack and Wimmer (2002) used an improved block-minimum method by implementing a hierarchical approach to detect non-ground raster elements.

Segmentation-based methods use grouped neighbour points which are generated by using some homogeneity criterion (Sithole 2005). Rather than classify individual points, segment-based methods classify segments into ground and non-ground objects by using the characteristics of the segment. Akel et al. (2005), Gorte (2002), and Lee and Schenk (2001) applied a region-growing approach to create segments and used the segments to classify lidar data. Jacobsen and Lohmann (2003) used the eCognition software (Definiens, Munich, Germany) to generate segments and classified segments into different types of objects, so that non-ground objects were filtered and only bare-ground remained to achieve DEM. Tovari and Pfeifer (2005) applied a robust interpolation-based filtering method using the segments which were created by the region-growing method rather than individual points.

Regardless of types of filtering methods, it is challenging to distinguish between ground returns and points reflected in the vegetation where there is a steep slope under dense forest cover (Kobler et al. 2007). This is because this type of area has sparse and spatially heterogeneous ground returns. In addition, due to a steep gradient in this type of area, slope-based threshold methods do not work properly (Sithole 2001). As raw lidar point data are normally processed in automated approaches due to large amounts of data, it is required to optimize filtering parameters with minimal user intervention (Kobler et al. 2007). Most existing filtering methods are based on the assumption that variations of natural terrain are more gradual than those of non-terrain surfaces. So, the majority of filtering methods calculate elevation differences and slope changes and determine certain threshold values for distinct points (Meng et al. 2009; Sithole and Vosselman 2004). Thus, it is necessary to gain prior knowledge of the sites to select threshold or parameter values. In addition, this assumption has shown limited success on steep and densely forested areas where the basic assumption often fails because of steep terrain gradients and sparse ground points.

The objective of this study is to develop a robust method that classifies raw lidar points into ground and non-ground points by using a progressive terrain fragmentation (PTF)

method which iteratively densifies a triangular surface by relatively robust criteria. This method is similar to that of Axelsson (2000). The uniqueness of our method is in prioritizing a set of lidar points, which are used to approximate a triangulated irregular network (TIN) surface so that more representative terrain points are included before the other points. This prioritization procedure minimizes the false inclusion of non-ground points during the iteration process.

2. Materials and methods

2.1. Progressive Terrain Fragmentation (PTF) algorithm

The characteristics of the TIN structure, which represents a surface as a set of non-overlapping contiguous triangular facets of irregular shape and size, are very effective in identifying subgroups of surfaces to represent heterogeneous terrain surfaces (Lee 1991). The seed point set is used to generate the initial terrain surface in a TIN structure, and additional terrain points are included at the end of each iteration for the following terrain estimation. The key requirement in this method is the setting up criteria to select correct terrain points. It is challenging to set-up criteria to filter out non-terrain points from the raw lidar point clouds for a large area of varied terrain characteristics. Although there are many studies on extraction of the terrain surface model from raw lidar points, there is much room for improving efficiency and accuracy of filtering methods with minimum user intervention (Liu 2008; Silvan-Cardenas and Wang 2006).

In this study, we first prepared multi-level local minimum point sets as candidate ground points from all raw lidar point clouds. Figure 2 shows an example of lidar point reduction at different levels. The maximum cell size (initial-level) and the finest cell size (ending-level) can be specified by the user's decision based on the characteristics of the site. From sparse point sets, the terrain approximation surface is estimated in a TIN structure. Then, the points are added to TIN estimation in each iteration, if the point satisfies the specified criteria. The criteria differ in characteristics of each triangular surface to give priority to more important (or significant) points to approximate the terrain surface, yet minimize commission errors. It is similar to the approach by Sohn and Dowman (2008), who classified TIN surfaces based on the characteristics of contained points. In our research, we classify TIN facets into convex (upward curved) and concave (downward curved) surfaces based upon the orthogonal distance between the facet and the points as follows. The lidar points falling into the same facet are grouped as the member points of the corresponding facet. The orthogonal distance between the TIN facet and candidate points are calculated. Then, if there is at least one negative point (a point which is below the TIN surface) in the member points, the surface is classified as a 'concave surface'. For concave surfaces (downward curved surfaces), the point with maximum distance in the negative direction (below the surface) from the facet surface is selected and added to terrain points. Otherwise, if there are only positive offset points (above the surface), it is classified as a 'convex surface'. For convex surfaces (upward curved surfaces), the point with the minimum angle (between a facet and a node point) within a certain threshold (α) is selected. Then the selected point is added to the set of ground points for the next iteration. The flowchart of progressive terrain fragmentation algorithm is illustrated in Figure 1.

2.1.1. Lidar point reduction

One of the most beneficial characteristics of lidar data is its high density and detail by a 3D point cloud. On one hand, extremely high sampling makes it possible to extract a broad

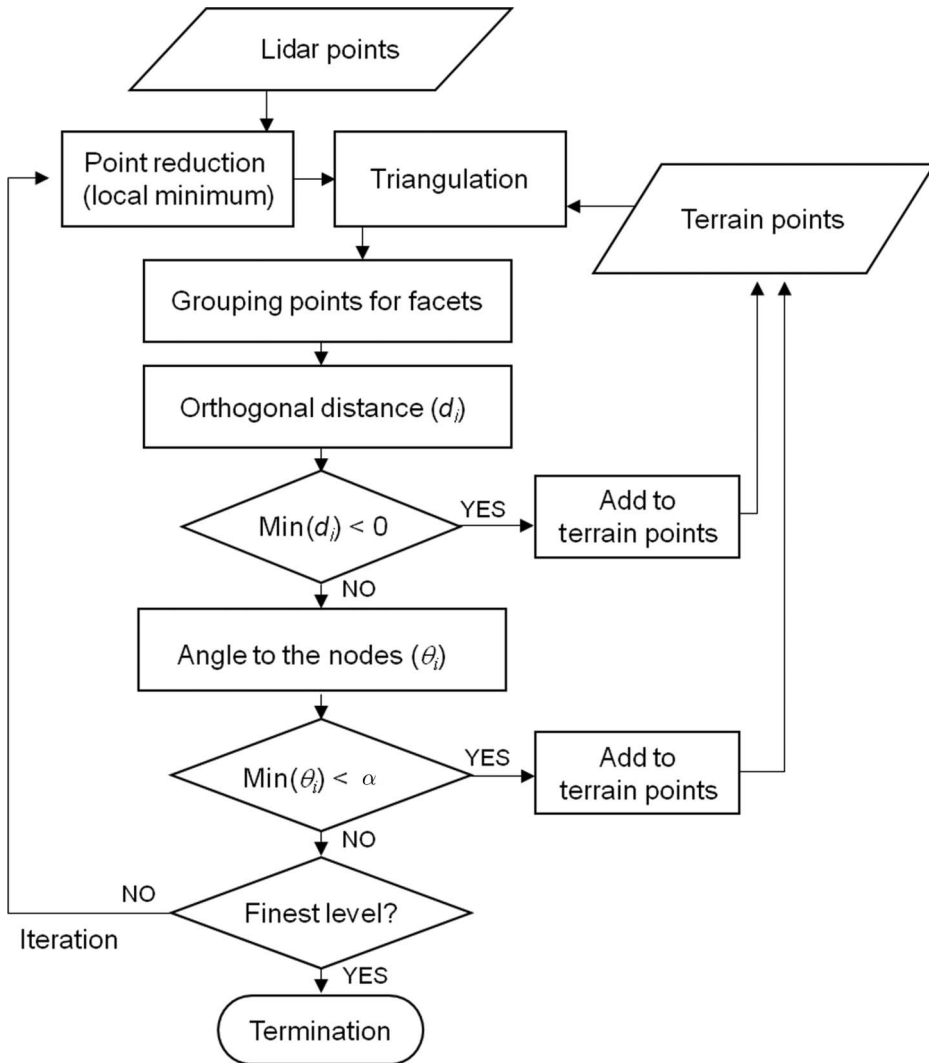


Figure 1. Flowchart of the Progressive Terrain Fragmentation algorithm.

range of useful information from the data sets. On the other hand, a large volume of data requires a lot of storage resource and processing power. The iterative process, especially, requires extensive processing time and power. In optimal conditions, higher lidar point density (sampling density) can provide more accurate surface description. However, because only a small part of all data points is returned from the terrain surfaces (especially, heterogeneous forested areas), processing all echoes would be inefficient when there is no accuracy improvement for retrieving terrain elevation models (Liu 2008).

In this research, we use a coarse-to-fine strategy, which starts with sparse points (broad scale) for an initial surface estimation and moves to the finer scale level for retrieving a real terrain surface by fragmenting triangular surfaces (Figure 2). The approach used by this study is similar to the progressive TIN densification method (Axelsson 2000) and recursive terrain fragmentation (Sohn and Dowman 2008). Although only a small fraction of lidar

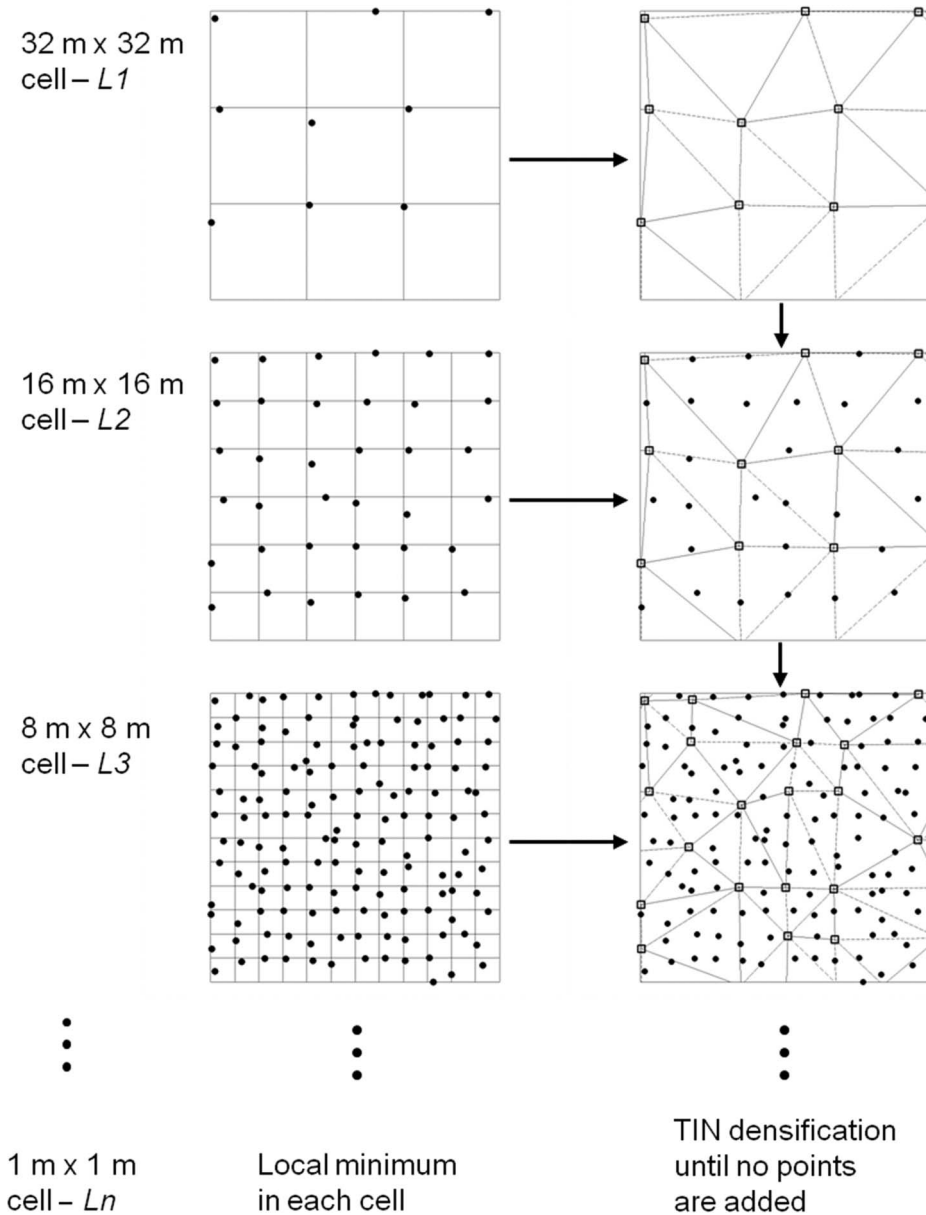


Figure 2. Example of lidar points reduction at different levels and TIN surface fragmentation.

points is selected and used for approximating the terrain surface at a coarse level of estimation, if all raw lidar points are used for the search process, the efficiency of the process is significantly decreased. To cope with this problem, multi-level point sets are generated so that reduced point sets are used for the coarse-scale stage and the next level of point sets (higher density) is used as the iteration continues. Local minimum elevation points are selected as candidate terrain points in the hierarchical configuration that follows. A non-overlapping grid with squared cells is superimposed over the original raw lidar points. The

minimum elevation value within each cell is selected as a candidate ground point. It starts from a $1\text{ m} \times 1\text{ m}$ sized cell and the size is doubled at each grid level until it reaches the maximum cell size, which can vary by user's decision. The maximum cell size is selected based on the largest type of structure in the area (Axelsson 2000). In this study, 32 m is selected for the maximum cell size because 32 m is large enough to filter out the largest type of object (i.e. trees). Even though the surface fragmentation process is performed from coarse to fine scale, searching for the minimum value at each level is carried out in reverse scale (fine to coarse strategy) because the minimum point at a certain level is one of the four minimum values of the previous finer level. For this reason, the number of points required for searching minimum elevation is decreased by 1/4 of the previous level.

2.1.2. Triangulation and assign point for each facet

An initial TIN surface is derived from the coarsest level of the point sets with a grid size of $L1$ (32 m). After that, the next level of point sets (extracted from a grid size of $L2$ (16 m)) is used to search terrain points. The points falling into the same facet are grouped and the points of each group are processed with the parameters calculated from the facet where the points belong. Instead of calculating all of the lidar points in each iteration step, coarse-to fine-scale levels of point sets are used. Figure 2 illustrates triangulation from the set of reduced lidar points.

2.1.3. Searching terrain points

We calculate the orthogonal distance between all of the member points falling into a certain triangle and the triangle plane. Each triangle is defined by three nodes (terrain points selected from previous approximation) so that each planar surface is modelled from these three points. Then, the characteristic of the triangle is classified as either a concave (downward curved) or convex (upward curved) surface as follows.

Concave: The orthogonal distance is calculated between a point (P_i) and the corresponding perpendicular point (P_i') on the plane. When the elevation of P_i is lower than P_i' ($z_i - z_i' < 0$), the orthogonal distance is negative and *vice versa*. If there is at least one negative offset point in a facet, it is classified as a concave facet (Figure 3(a)). Then, a point with the minimum offset height (maximum distance in a negative direction from the facet) is searched within a specific facet and the selected point is added to the terrain point set (Figure 3(b)). These points, classified as terrain points, are used for creating the new surface at the next iteration.

Convex: A facet with no negative offset point is classified as a convex surface (Figure 3(c)). In this case, the point with the minimum divergent angle (within a threshold angle – admissible angle (α)) is selected as a terrain point. For searching the minimum angular divergent point, we calculate angles between the node and the facet. Because there are three angles between one node and a TIN facet (tetrahedral shape), we select the maximum angle (out of three angles) as a representing angle ($\theta_i = \text{MAX}(\theta_{i1}, \theta_{i2}, \theta_{i3})$). Once the representative angle is determined for each point, we select the minimum angular divergent point among the points falling into a certain TIN facet. Then, we use this angle for assessing whether it is a ground or non-ground point in the filtering procedure (Figure 3(d)). The purpose of using the minimum divergent point for convex surfaces is to minimize the possibility of commission errors (classifying non-ground point as ground points incorrectly). In this iterative procedure, commission errors could lead to large propagated errors if falsely created terrain surfaces are used as a basis for the following raw point assessment.

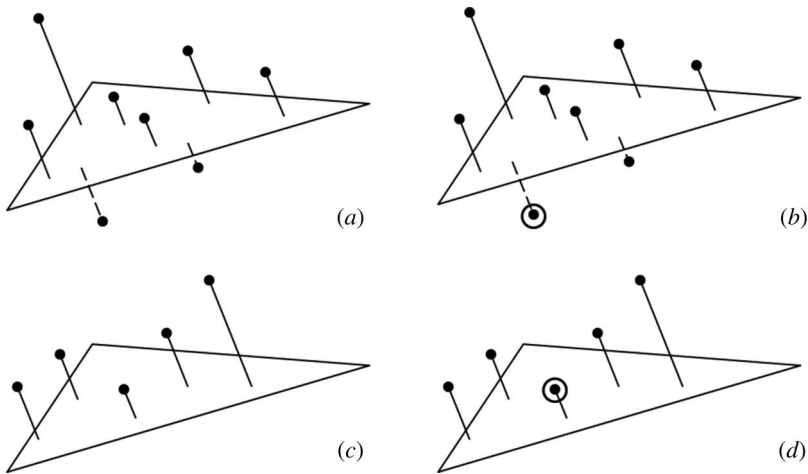


Figure 3. Illustration of triangular surface types and searching terrain points. (a) Concave surface, (b) selecting the maximum distance offset point in negative direction, (c) convex surface, and (d) searching the minimum angle point within admissible angle range.

We iteratively conduct this terrain point-searching procedure until no additional terrain point exists for each level. Then, the search moves to the next level (coarse to fine scale) and repeats the procedure.

2.1.4. Lidar points classification

It is common to interpolate raw lidar points into raster images before applying filtering procedures because filtering on raster images runs faster than processing raw lidar point clouds (Chen 2007). However, interpolating lidar points into raster images causes loss of information (Liu 2008). Therefore, instead of converting lidar point into raster images, all lidar points are explicitly classified into either ground points or non-ground points. The terrain surface which is created at the end of the iteration is used as the basis for point classification. If the orthogonal distance is less than 0.3 m, these points are classified as ground points and others are assigned as non-ground points. Offset distance threshold was selected by doubling typical vertical accuracy of the ALTM 1233 laser mapping system (Optech Inc., Ontario, Canada) (15 cm) (International Hurricane Research Center 2012). These classified points are compared to the reference plot data sets and are used for final accuracy assessment.

2.2. Test site and data

2.2.1. Test site

To evaluate this method, we perform our analysis at the Angelo Reserve (39° 45' N; 123° 38' W; 430–1290 m elevation), which is part of the University of California Natural Reserve System (NRS) in Mendocino County, CA. This site is particularly useful for our purpose (evaluating the performance of a non-terrain filtering method) because this area consists of heterogeneous forests with various densities and a steep topographic slope. In other words, the site represents difficult conditions for separating ground and non-ground

points from raw lidar data in automated procedures. In north-facing slopes, old conifer species are dominant (*Pseudotsuga*) and are mixed with broadleaf trees (*Lithocarpus*). *Quercus* species (*Pseudotsuga*-mixed hardwood forest), and to a lesser extent tanoak, are present as well (Hunter and Barbour 2001; Power et al. 2004). We use a study site of size 4 km², which is a subset of the entire data set (180 km²) of the South Fork Eel river watershed.

2.2.2. Lidar data

Lidar data used in this study were generated by the National Science Foundation (NSF)-supported National Center for Airborne Laser Mapping (NCALM). Airborne laser scanning was performed on 29 June 2004. The data were acquired by an ALTM 1233 laser mapping system (Optech Inc.) mounted on a fixed-wing aeroplane. The mean flying altitude was 600 m above the ground. The laser pulse frequency was 33 kHz and the scanning frequency was 28 Hz. The swath width was 20° per half angle and 50% overlapping flight lines were used. The data sets included the first and last pulses for *x*, *y*, *z* coordinates, intensity value, and GPS (global positioning system) time. Combined with inertial navigation and kinematic GPS, this system provides absolute elevation of the ground surface with vertical accuracy of 10–15 cm in open areas (Farid et al. 2008; International Hurricane Research Center 2012). The density of lidar points is varied by flight height, ground surface elevation changes, and overlap between swaths. The average point density of this study is 3.1 echoes per square metre (first and last returns combined).

2.2.3. Reference plots

Because the main objective of this study is to separate ground and non-ground points from raw lidar point clouds, the performance is accessed by accuracy of filtering non-ground points rather than absolute elevation errors. Several research studies conducted field measurement of reference points with a combination of total station and GPS units (Hodgson and Bresnahan 2004; Kobler et al. 2007; Reutebuch et al. 2003; Bater and Coops 2009).

Sithole and Vosselman (2004) create the reference data for their comparison of filter algorithms by the manual point interpretation method. In addition, Kobler et al. (2007) suggest that manual filtering is the best possible method, given no additional information. Accordingly, we manually create the reference data from the original lidar point cloud. Because point density is high enough to depict ground surface and non-ground objects (e.g. tall trees and sub-canopy vegetation), we are able to create reference data by manual interpretation of 3D lidar point plots. Non-ground points are carefully selected and removed by 3D visualization software (Quick Terrain Modeler, Applied Imagery). By this visual interpretation procedure, all points are explicitly assigned as either 'ground points' or 'non-ground points' and are used for selecting optimal parameters and assessing performance of this method. Even though we are familiar with this area, it is impossible to discover the pattern of lidar point distribution over the entire area before analysing the data sets. Thus, we place 16 reference plots (10 m × 10 m) systematically. The distance between plots is set to 200 m in two perpendicular directions (either north–south or east–west), so that plots are well distributed over the study site. Figure 4 shows the distribution of 16 reference plots.

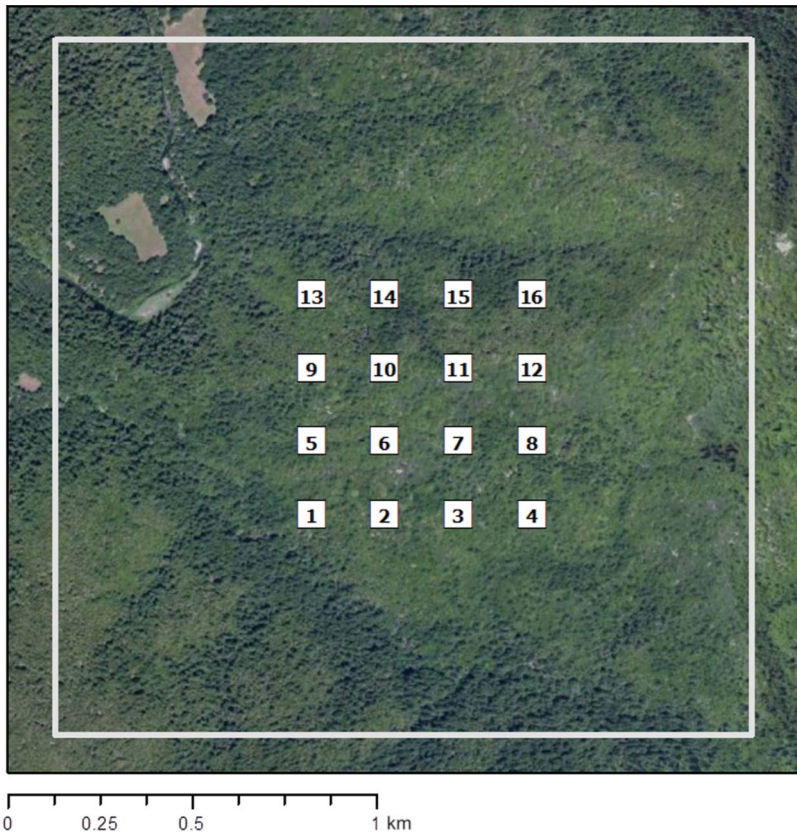


Figure 4. Reference plots (10 m \times 10 m) in test area (4 km²).

2.3. DEM for qualitative analysis

Although the main purpose of this study is to classify raw lidar points into ground and non-ground points, we additionally generate a DEM for visual inspection of classification quality. Because a continuous surface is easier for the human eye to detect abnormal shapes, an interpolated surface is utilized to identify inaccurate lidar point filtering results. Evans and Hudak (2007) suggest that thin-plate interpolation provides a better result than others, such as ordinary kriging and inverse distance weighting. Accordingly, we use thin-plate interpolation (TPI) for interpolating terrain point and creating DEM for visualizing terrain surfaces.

2.4. Parameter optimization

The PTF method requires three parameters: (1) angle threshold between a triangular surface and a node point, (2) distance threshold, and (3) grid size for initial seed points. Because distance threshold is intended to remove only outliers (either positive or negative), it does not have a huge impact if there is no outlier in the raw lidar points. We used 100 m as a threshold value for both positive and negative direction. Also, the result is not sensitive to the grid size for the initial seed points. A grid size for initial seed points can be selected based on the largest non-ground object (e.g. building) within the filtering area (Axelsson 2000). In this

study, there is no large artificial object in the filtering area, so a value is set to 32 m, which is larger than the canopy diameter of tall trees. Angle threshold is the key parameter to decide the performance of this method. It is important to determine an adequate threshold value to maximize filtering performance. In this study, we use 16 systematically distributed plots to assess the performance of this method.

The optimal threshold (admissible angle) value is selected by comparing percentage errors between different threshold values. For a quantitative analysis of this method, the filtering errors, which are produced by comparing the filtering result with the reference data, are investigated. There are two types of errors in filtering lidar data – Type I (omission) error and Type II error (commission). A Type I error is to miss ground points even though the points are truly ground points, and a Type II error is to falsely classify non-ground points as ground points. Total errors can represent combined error (Type I and Type II). However, it is considered that the total number of errors is greatly influenced by the proportion between ground and non-ground points (Sithole and Vosselman 2004).

3. Results

3.1. Parameter selection

As we describe above, the main parameter to determine the accuracy of this method is angle threshold. We test different admissible angles to decide the optimum angular threshold value. As the admissible angle increases, Type II errors (falsely accepting non-ground points as ground points) increase, but Type I errors (misclassifying true ground points as object points) decrease and *vice versa*. Depending on the priority in filtering purpose, the balance between Type I and Type II errors can be adjusted. For example, minimizing Type II errors intends to remove as many non-ground points as possible, so that a terrain model from ground points does not create false peaks and spikes. However, it compromises the detail of the terrain surface by removing true ground points. Because the two error types react in an opposite manner, a total error can be used to assess the performance of certain methods. Figure 5 shows total, Type I, and Type II errors at different admissible angles (from 15° to 20°). The minimum total error is acquired at the angle value of 18°. Table 1 shows the confusion matrix with an angle threshold of 18° (all 16 plots combined); 10.7% of ground points (48 out of 448) were misclassified as non-ground points (Type I error) and 0.72% of non-ground points (35 out of 4893) were falsely classified as ground points (Type II error). The total error is 1.55% and the total error is mostly influenced by Type II error because non-ground points comprise a large proportion of all plots. Figure 6 shows the different results obtained for various admissible angles. When the admissible angle of 15° was used, a large portion of true ground points was removed because the ground points were misclassified as non-ground points.

3.2. Error analysis by plot characteristics

Although the plots are selected by a systematic sampling scheme, the reference plots represent different surface shape characteristics so that we can recognize the source of errors and optimize the threshold value under different surface characteristics. Table 2 shows total, type I, and type II error for the 16 reference plots.

A Type I error at Plot 9 is 95.3% with 15° angle threshold and the error is changed to 25.6% with a 20° angle threshold. Because Plot 9 is located on a steep ridge line, a small angle threshold is not able to detect ground points during iteration procedures; so,

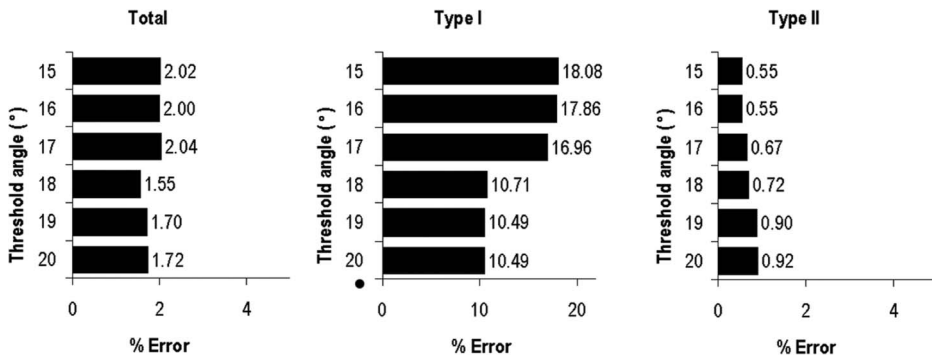


Figure 5. Results of total, Type I, and Type II errors at different admissible angles.

Table 1. Accuracy assessment table (angle threshold: 18°).

		Filtered		Total points	Error	
		BE	OBJ		Type	%
Ref.	BE	400	48	448	I	10.71%
	OBJ	35	4858	4893	II	0.72%
	Total	435	4906	5341	Total	1.55%

Note: BE, bare earth; OBJ, object.

this plot shows a large type I error at the low-angle threshold. We find that a value of 18° is the minimum threshold to retrieve correct terrain shapes for this plot. Plot 1 and Plot 10 show similar results (with less magnitude) because both plots are also on ridge lines. For Plots 4 and 12, Type II errors increased as angle threshold increased. These plots have relatively low vegetation, so it is more likely to falsely detect non-terrain (low vegetation) as terrain points. Other plots (2, 3, 5–8, 11, 13–16) are not sensitive to angle threshold and show almost the same number of errors, regardless of error types. This is because these plots have large gaps between terrain surfaces and canopy layers (tall trees), and hence the confusion between ground and non-ground points is less likely to happen.

3.3. Qualitative assessment of filtering performance

In addition to the quantitative analysis of the contingency matrix with 16 reference plots, we also perform qualitative analysis by visual inspection of the interpolated DEM. Reference plots are responsible for the accuracy of our method, the plots are discrete and are simply a smaller portion of the entire study area. Hence, visual inspection of the interpolated ground surface (i.e. DEM) from the lidar points, which are classified as ground points, supplements the limitation of the quantitative accuracy assessment (plot-based approach). Figure 7 shows the DEM created from ground points for qualitative analysis. By using a hillshading map from the DEM, we visualize the 3D characteristics of the created DEM. The angle threshold value is set to 18°, which is acquired from previous procedures. This angle threshold is large enough to remove all major Type I errors (omission errors) in the area, and hence we cannot detect major loss of terrain surface description. However, it falsely classifies low vegetation points as ground points, and we can detect commission errors at south-facing slopes covered with low vegetation.

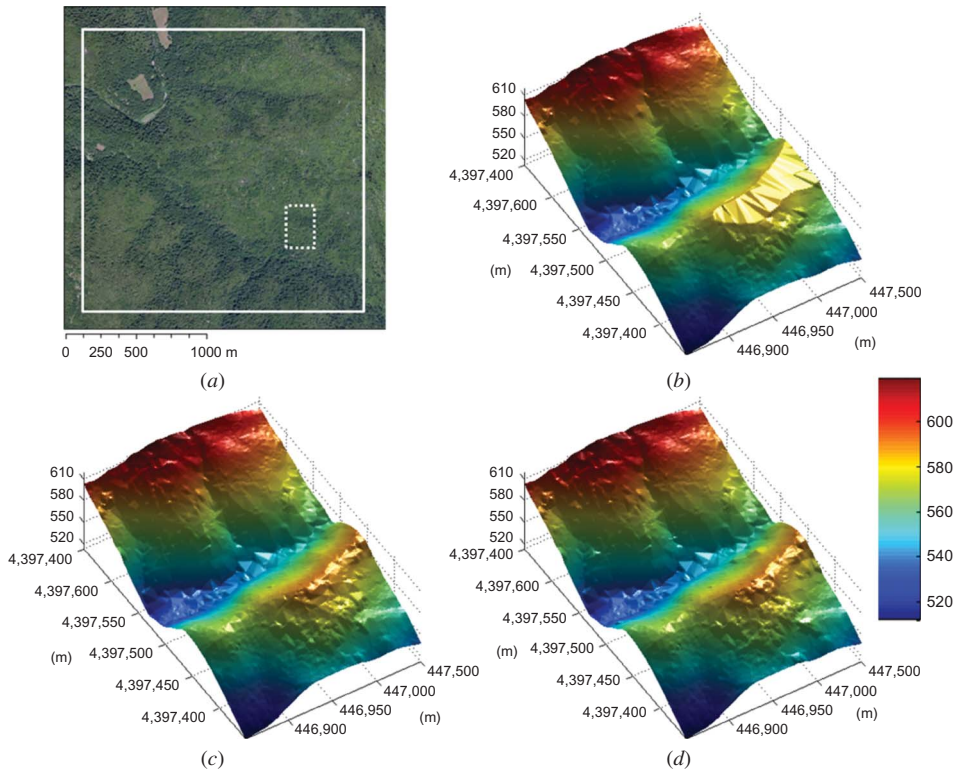


Figure 6. DEM created by different admittance angles for the subset area. (a) Location of the subset area, (b) admittance angle 15° , (c) admittance angle 18° , and (d) admittance angle 20° .

4. Discussion

By using point data rather than interpolated surface for separating ground and non-ground points, we minimize the errors during the interpolation of lidar points to a raster surface. In general, approaches that use raw lidar points require more computing power; so these approaches are slower than the raster-based approaches. However, we use a coarse-to-fine approach to select ground points from the raw lidar point clouds so that relatively small numbers of points are used at each iteration. Hence, we expect that this approach would provide faster performance than the methods that utilize all lidar points throughout a procedure. In addition, we prioritize a set of lidar points, which are used to approximate a TIN surface so that important terrain points are added earlier than the other points.

While our approach to classify the ground and non-ground points from the raw lidar points for complex forested areas has advantages, there are still several aspects which need to be improved. The result from our study shows that one universal threshold value cannot perform optimally for all types of terrain characteristics. Even though a threshold value can be adjusted by a user's preferences, more study should be conducted to optimize a threshold value with minimum user interventions. The major limitation of our method is the use of one universal threshold value for the entire level of filtering procedures. We found that different threshold values are required for different levels of scale (especially coarse- to fine-scale approaches). For example, relatively large threshold values are needed only for

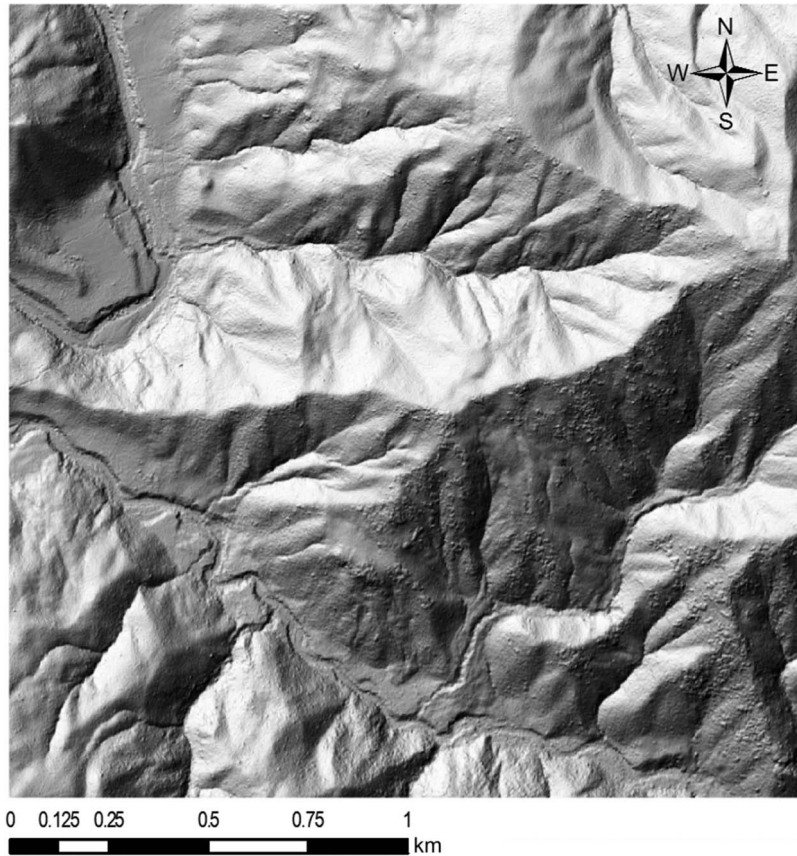


Figure 7. Shaded relief map of DEM by 18° angle threshold (1 m grid cell size, thin-plate interpolation).

the early stage of terrain approximation so as not to omit terrain points, and smaller threshold values are preferred to reduce commission errors (falsely detect low object points as terrain points). In addition, our approach showed limited success in separating ground and non-ground points when the area is covered by low and dense vegetation. This limitation is mainly caused by the characteristics of discrete-return lidar systems, which do not have sufficiently short pulse width to record ground return pulses when the ground is covered by low vegetation. Hence, it is recommended to understand this limitation before applying our approach.

Although this method has been developed for complex forested areas with steep terrain slopes, we need to test the performance of this method for different environmental conditions. For example, under urban conditions, which have various types of artificial structures (buildings, bridges, ditches), the parameters should be tested and may need to be optimized to maximize the accuracy of the results.

Also, for more objective comparison with other filtering methods, we need to perform our method with a common data set and reference data, such as the International Society for Photogrammetry and Remote Sensing (ISPRS) Commission III/WG3 data set (Sithole and Vosselman 2004). Because the ISPRS data set has various site conditions, we

can test our method for different environmental conditions. In addition, we can directly compare the performance and accuracy of our method with the previously conducted studies.

It is worth mentioning that the development of filtering methods is closely related to the advancement of airborne laser-sensing technology. Although conventional discrete return airborne laser scanning systems have provided unprecedented high-quality data sets for research pertaining to land surface processes (Slatton et al. 2007; Carter, Shrestha, and Slatton 2007), discrete return scanning systems provide discrete pulses separated by several metres due to the pulse width (length). In general, the pulse width of lidar systems ranges from 6 to 12 ns, which translates into pulse lengths of 1.8–3.6 m (Hodgson et al. 2003). Hence, conventional discrete lidar sensors have difficulties in filtering off-ground points where low vegetation exists on steep slopes and abrupt changes take place (Lin and Mills 2009; Raabe et al. 2008). Recently, full-waveform scanning systems are becoming more popular because full-waveform scanning systems provide additional attributes (such as amplitude and echo width) over conventional discrete return systems for extracting terrain surface (Mallet and Bretar 2009; Rutzinger et al. 2008). Lin and Mills (2009) applied the progressive densification filter developed by Axelsson (2000) with full-waveform scanning systems to improve the accuracy for extracting DTM. Doneus et al. (2008) also took advantage of a full-waveform scanning system to separate low-level vegetation from the ground for archaeological application.

5. Conclusion

In this study, the PTF method is developed to improve the performance of filtering non-terrain points from raw airborne laser scanning data. Iterative procedures for searching terrain points gradually approximates terrain surface. Instead of using absolute slope or offset distance, this method utilizes orthogonal distance and relative angle between a triangular plane and a node. For this reason, PTF was able to classify raw lidar points into ground and non-ground points on a heterogeneous steep forested area with a small number of parameters. We found that ‘admissible angle’ is the most influential parameter for accurate filtering procedures, and a smaller admissible angle threshold causes inaccurate terrain approximation by omitting terrain points around ridge lines. On the contrary, a large admissible angle threshold is associated with failure to remove low vegetation. The optimum threshold value for admissible angle was selected by examining 16 reference plots, which minimizes the total number of errors for classifying raw lidar points. Classifying raw lidar points (ground vs non-ground) for generating terrain surface is a basis for other analyses related to forest biophysical parameter extraction. Thus, we expect that our study will provide more accurate terrain approximation and contribute to improving extraction of other forest biophysical parameters.

Acknowledgement

We gratefully acknowledge the use of lidar data sets supplied by Dr William E. Dietrich and the National Center of Airborne Laser Mapping (NCALM). J.H. Lee was funded by the W.S. Rosecrans Fellowship, Environmental Science, Policy, and Management, University of California, Berkeley. Dr Joshua B. Fisher contributed to this paper through work in the Jet Propulsion Laboratory, California Institute of Technology, under a contract with the National Aeronautics and Space Administration.

References

- Akel, A. N., K. Kremer, S. Filin, M. Sester, and Y. Doytsher. 2005. "Dense DTM Generalization Aided by Roads Extracted from LiDAR Data." *International Archives of Photogrammetry and Remote Sensing*, Vol. 36-3/W19, Enschede, September 12–14, 54–59.
- Asner, G. P., J. Mascaro, H. C. Muller-Landau, G. Vieilledent, R. Vaudry, M. Rasamoelina, J. S. Hall, and M. Breugel. 2011. "A Universal Airborne LiDAR Approach for Tropical Forest Carbon Mapping." *Oecologia* 168: 1147–1160.
- Axelsson, P. 2000. "DEM Generation from Laser Scanner Data Using Adaptive TIN Models." *International Archives of Photogrammetry and Remote Sensing*, Vol. 33, Part B4, Amsterdam, July 16–23, 110–117.
- Bater, C. W., and N. C. Coops. 2009. "Evaluating Error Associated with Lidar-Derived DEM Interpolation." *Computers & Geosciences* 35: 289–300.
- Carter, W. E., R. L. Shrestha, and K. C. Slatton. 2007. "Geodetic Laser Scanning." *Physics Today* 60: 41–46.
- Chen, Q. 2007. "Airborne Lidar Data Processing and Information Extraction." *Photogrammetric Engineering and Remote Sensing* 73: 109–112.
- Clark, M. L., D. B. Clark, and D. A. Roberts. 2004. "Small-Footprint Lidar Estimation of Sub-Canopy Elevation and Tree Height in a Tropical Rain Forest Landscape." *Remote Sensing of Environment* 91: 68–89.
- Clark, M. L., D. A. Roberts, J. J. Ewel, and D. B. Clark. 2011. "Estimation of Tropical Rain Forest Aboveground Biomass with Small-Footprint Lidar and Hyperspectral Sensors." *Remote Sensing of Environment* 115: 2931–2942.
- Cobby, D. M., D. C. Mason, and I. J. Davenport. 2001. "Image Processing of Airborne Scanning Laser Altimetry Data for Improved River Flood Modelling." *ISPRS Journal of Photogrammetry and Remote Sensing* 56: 121–138.
- Doneus, M., C. Briese, M. Fera, and M. Janner. 2008. "Archaeological Prospection of Forested Areas Using Full-Waveform Airborne Laser Scanning." *Journal of Archaeological Science* 35: 882–893.
- Evans, J. S., and A. T. Hudak. 2007. "A Multiscale Curvature Algorithm for Classifying Discrete Return LiDAR in Forested Environments." *IEEE Transactions on Geoscience and Remote Sensing* 45: 1029–1038.
- Farid, A., D. C. Goodrich, R. Bryant, and S. Sorooshian. 2008. "Using Airborne Lidar to Predict Leaf Area Index in Cottonwood Trees and Refine Riparian Water-Use Estimates." *Journal of Arid Environments* 72: 1–15.
- Gorte, B. 2002. "Segmentation of TIN-Structured Surface Models." *International Archives of Photogrammetry Remote Sensing and Spatial Information Sciences* 34: 465–469.
- Habib, A., M. Ghanma, M. Morgan, and R. Al-Ruzouq. 2005. "Photogrammetric and Lidar Data Registration Using Linear Features." *Photogrammetric Engineering and Remote Sensing* 71: 699–707.
- Hodgson, M. E., and P. Bresnahan. 2004. "Accuracy of Airborne Lidar-Derived Elevation: Empirical Assessment and Error Budget." *Photogrammetric Engineering and Remote Sensing* 70: 331–339.
- Hodgson, M. E., J. R. Jensen, L. Schmidt, S. Schill, and B. Davis. 2003. "An Evaluation of LIDAR- and IFSAR-Derived Digital Elevation Models in Leaf-on Conditions with USGS Level 1 and Level 2 DEMs." *Remote Sensing of Environment* 84: 295–308.
- Hunter, J. C., and M. G. Barbour. 2001. "Through-Growth by Pseudotsuga Menziesii: A Mechanism for Change in Forest Composition Without Canopy Gaps." *Journal of Vegetation Science* 12: 445–452.
- Hyypä, J., H. Hyypä, D. Leckie, F. Gougeon, X. Yu, and M. Maltamo. 2008. "Review of Methods of Small-Footprint Airborne Laser Scanning for Extracting Forest Inventory Data in Boreal Forests." *International Journal of Remote Sensing* 29: 1339–1366.
- International Hurricane Research Center. 2012. "Airborne Laser Technology." Accessed October 8. http://www.ihc.fiu.edu/lcr/research/airborne_laser_mapping/
- Jacobsen, K., and P. Lohmann. 2003. "Segmented Filtering of Laser Scanner DSMs." *International Archives of Photogrammetry and Remote Sensing*, Vol. 36, Dresden, October 8–10, 87–93.
- Jensen, J. L. R., K. S. Humes, T. Conner, C. J. Williams, and J. DeGroot. 2006. "Estimation of Biophysical Characteristics for Highly Variable Mixed-Conifer Stands Using Small-Footprint Lidar." *Canadian Journal of Forest Research-Revue Canadienne De Recherche Forestiere* 36: 1129–1138.

- Kilian, J., N. Haala, and M. Englich. 1996. "Capture and Evaluation of Airborne Laser Scanner Data." *International Archives of Photogrammetry and Remote Sensing*, Vol. 31, Part B3, Vienna, July 12–18, 383–388.
- Kobler, A., N. Pfeifer, P. Ogrinc, L. Todorovski, K. Oštir, and S. Džeroski. 2007. "Repetitive Interpolation: A Robust Algorithm for DTM Generation from Aerial Laser Scanner Data in Forested Terrain." *Remote Sensing of Environment* 108: 9–23.
- Kraus, K., and N. Pfeifer. 1998. "Determination of Terrain Models in Wooded Areas with Airborne Laser Scanner Data." *ISPRS Journal of Photogrammetry and Remote Sensing* 53: 193–203.
- Lee, A. C., and R. M. Lucas. 2007. "A LiDAR-Derived Canopy Density Model for Tree Stem and Crown Mapping in Australian Forests." *Remote Sensing of Environment* 111: 493–518.
- Lee, H. S., and N. H. Younan. 2003. "DTM Extraction of Lidar Returns via Adaptive Processing." *IEEE Transactions on Geoscience and Remote Sensing* 41: 2063–2069.
- Lee, I., and T. Schenk. 2001. "3D Perceptual Organization of Laser Altimetry Data." *International Archives of Photogrammetry and Remote Sensing*, Vol. 34-3/W4, Annapolis, MD, October 22–24, 57–65.
- Lee, J. 1991. "Comparison of Existing Methods for Building Triangular Irregular Network Models of Terrain from Grid Digital Elevation Models." *International Journal of Geographical Information Systems* 5: 267–285.
- Lefsky, M. A., W. B. Cohen, G. G. Parker, and D. J. Harding. 2002. "Lidar Remote Sensing for Ecosystem Studies." *Bioscience* 52: 19–30.
- Lim, K., P. Treitz, M. Wulder, B. St-Onge, and M. Flood. 2003. "LiDAR Remote Sensing of Forest Structure." *Progress in Physical Geography* 27: 88–106.
- Lin, Y. C., and J. Mills. 2009. "Integration of Full-Waveform Information into the Airborne Laser Scanning Data Filtering Process." *International Archives of Photogrammetry and Remote Sensing*, Vol. 38-3/W8, Paris, September 1–2, 224–229.
- Liu, X. Y. 2008. "Airborne LiDAR for DEM Generation: Some Critical Issues." *Progress in Physical Geography* 32: 31–49.
- Mallet, C., and F. Bretar. 2009. "Full-Waveform Topographic Lidar: State-of-the-Art." *ISPRS Journal of Photogrammetry and Remote Sensing* 64: 1–16.
- Meng, X. L., L. Wang, J. L. Silvan-Cardenas, and N. Currit. 2009. "A Multi-Directional Ground Filtering Algorithm for Airborne LIDAR." *ISPRS Journal of Photogrammetry and Remote Sensing* 64: 117–124.
- Næsset, E., T. Gobakken, J. Holmgren, H. Hyypä, J. Hyypä, M. Maltamo, M. Nilsson, H. Olsson, Å. Persson, and U. Söderman. 2004. "Laser Scanning of Forest Resources: The Nordic Experience." *Scandinavian Journal of Forest Research* 19: 482–499.
- Popescu, S. C. 2007. "Estimating Biomass of Individual Pine Trees Using Airborne Lidar." *Biomass & Bioenergy* 31: 646–655.
- Power, M. E., W. E. Rainey, M. S. Parker, J. L. Sabo, A. Smyth, S. Khandwala, J. C. Finlay, F. C. McNeely, K. Marsee, and C. Anderson. 2004. "River-to-Watershed Subsidies in an Old-Growth Conifer Forest." In *Food Webs at the Landscape Level*, edited by G. A. Polis, M. E. Power, and G. Huxel, 217–240. Chicago, IL: University of Chicago Press.
- Raabe, E. A., M. S. Harris, R. L. Shrestha, and W. E. Carter. 2008. Derivation of Ground Surface and Vegetation in a Coastal Florida Wetland with Airborne Laser Technology. Saint Petersburg, FL: US Geological Survey. Open-File Report 2008–1125.
- Reutebuch, S. E., R. J. McGaughey, H. E. Andersen, and W. W. Carson. 2003. "Accuracy of a High-Resolution Lidar Terrain Model Under a Conifer Forest Canopy." *Canadian Journal of Remote Sensing* 29: 527–535.
- Rutzinger, M., B. Höfle, M. Hollaus, and N. Pfeifer. 2008. "Object-Based Point Cloud Analysis of Full-Waveform Airborne Laser Scanning Data for Urban Vegetation Classification." *Sensors* 8: 4505–4528.
- Silvan-Cardenas, J. L., and L. Wang. 2006. "A Multi-Resolution Approach for Filtering LiDAR Altimetry Data." *ISPRS Journal of Photogrammetry and Remote Sensing* 61: 11–22.
- Sithole, G. 2001. "Filtering of Laser Altimetry Data Using a Slope Adaptive Filter." *International Archives of Photogrammetry Remote Sensing and Spatial Information Sciences* 34: 203–210.
- Sithole, G. 2005. "Segmentation and Classification of Airborne Laser Scanner Data." PhD diss., University of Delft.

- Sithole, G., and G. Vosselman. 2004. "Experimental Comparison of Filter Algorithms for Bare-Earth Extraction from Airborne Laser Scanning Point Clouds." *ISPRS Journal of Photogrammetry and Remote Sensing* 59: 85–101.
- Slatton, K. C., W. E. Carter, R. L. Shrestha, and W. Dietrich. 2007. "Airborne Laser Swath Mapping: Achieving the Resolution and Accuracy Required for Geosurficial Research." *Geophysical Research Letters* 34: L23S10.
- Sohn, G., and I. J. Dowman. 2008. "A Model-Based Approach for Reconstructing a Terrain Surface from Airborne Lidar Data." *Photogrammetric Record* 23: 170–193.
- Suarez, J. C., C. Ontiveros, S. Smith, and S. Snape. 2005. "Use of Airborne LiDAR and Aerial Photography in the Estimation of Individual Tree Heights in Forestry." *Computers & Geosciences* 31: 253–262.
- Tovari, D., and N. Pfeifer. 2005. "Segmentation Based Robust Interpolation – A New Approach to Laser Data Filtering." *International Archives of Photogrammetry, Remote Sensing*, Vol. 36, Enschede, September 12–14, 79–84.
- Vosselman, G. 2000. "Slope Based Filtering of Laser Altimetry Data." *International Archives of Photogrammetry and Remote Sensing* 33: 935–942.
- Wack, R., and A. Wimmer. 2002. "Digital Terrain Models from Airborne Laserscanner Data – A Grid Based Approach." *International Archives of Photogrammetry Remote Sensing and Spatial Information Sciences* 34: 293–296.
- Wulder, M. A., C. W. Bater, N. C. Coops, T. Hilker, and J. C. White. 2008. "The Role of LiDAR in Sustainable Forest Management." *Forestry Chronicle* 84: 807–826.
- Zhang, K., and D. Whitman. 2005. "Comparison of Three Algorithms for Filtering Airborne Lidar Data." *Photogrammetric Engineering and Remote Sensing* 71: 313–324.
- Zhang, K., S. C. Chen, D. Whitman, M. L. Shyu, J. Yan, and C. Zhang. 2003. "A Progressive Morphological Filter for Removing Nonground Measurements from Airborne LIDAR Data." *IEEE Transactions on Geoscience and Remote Sensing* 41: 872–882.